

Imaging the Expanding Shell of SN 2011dh

A. de Witt,^{1*} M. F. Bietenholz,^{1,2} A. Kamble,⁵ A. M. Soderberg,⁵ A. Brunthaler,³
B. Zauderer,⁵ N. Bartel,² and M. P. Rupen,⁴

¹*Hartebeesthoek Radio Observatory, PO Box 443, Krugersdorp, 1740, South Africa*

²*Department of Physics and Astronomy, York University, Toronto, M3J 1P3, Ontario, Canada*

³*Max-Planck-Institut für Radioastronomie, Auf dem Hügel 69, 53121 Bonn, Germany*

⁴*National Radio Astronomy Observatory, 1003 Lopezville Road, Socorro, NM 87801, USA*

⁵*Harvard-Smithsonian Center for Astrophysics, 60 Garden Street, Cambridge, MA 02138, USA*

ABSTRACT

We report on third epoch VLBI observations of the radio-bright supernova SN 2011dh located in the nearby galaxy (7.8 Mpc) M51. The observations took place at $t = 453$ d after the explosion and at a frequency of 8.4 GHz. We obtained a fairly well resolved image of the shell of SN 2011dh, making it one of only six recent supernovae for which resolved images of the ejecta are available. By fitting a spherical shell model directly to the visibility measurements we determine the angular radius of SN 2011dh’s radio emission to be $636 \pm 29 \mu\text{as}$. At a distance of 7.8 Mpc, this angular radius corresponds to a linear radius of $(7.4 \pm 0.3) \times 10^{16}$ cm and an average expansion velocity since the explosion of 18900_{-2400}^{+2800} km s⁻¹. We also calculated more precise radius measurements for the earlier VLBI observations and we show that all the measured values of the radius of the emission region, up to $t = 453$ d, are still almost perfectly consistent with those derived from fitting synchrotron self-absorbed models to the radio spectral energy distribution. We find that SN 2011dh’s radius evolves in a power-law fashion, with $R \sim t^{0.961 \pm 0.011}$, implying almost free expansion.

Key words: supernovae: individual (SN2011dh) — radio continuum: general.

1 INTRODUCTION

Supernova (SN) 2011dh, discovered in the “Whirlpool Galaxy”, M51, is a recent example of a radio-loud SN. At a distance of $7.8_{-0.9}^{+1.1}$ Mpc¹ (Ergon et al. 2014), SN 2011dh is also one of the nearest SNe observed in recent years. SN 2011dh was discovered on 2011 May 31 by the amateur astronomer Amádée Riou (Griga et al. 2011) and pre- and post-discovery imaging observations to confirm the discovery followed soon afterwards (Griga et al. 2011). The SN was coincident with the eastern spiral arm of M51. The explosion date is tightly constrained to be between 2011 May 31.275 and 31.893 UT (Arcavi et al. 2011). We will adopt the (rounded) midpoint of this interval, May 31.6 UT, as the explosion date, t_0 , and take t to be the age of the SN since the explosion.

Initially, SN 2011dh was spectroscopically classified as Type IIP (Silverman, Filippenko & Cenko 2011), but fur-

ther spectroscopy, which showed helium absorption features, caused a re-classification as a Type IIb (Arcavi et al. 2011; Marion et al. 2011). A maximum expansion velocity of ~ 20000 km s⁻¹ was estimated from the blue edge of the H α line (Silverman, Filippenko & Cenko 2011; Arcavi et al. 2011; Marion et al. 2014).

Radio emission was detected only a few days after the explosion, at centimeter wavelengths (Horesh et al. 2011) with the National Radio Astronomy Observatory² (NRAO) Karl G. Jansky Very Large Array (VLA), as well as at millimeter wavelengths (Horesh, Zauderer & Carpenter 2011) using the Combined Array for Research in Millimeter-wave Astronomy, and at submillimeter wavelengths (Soderberg et al. 2012) using the Submillimeter Array (SMA). The initial radio and millimeter-band observations were presented in Soderberg et al. (2012), while further broad-band measurements of the total radio flux density as well as modeling of the lightcurve are presented in Krauss et al. (2012).

A yellow supergiant which was visible in pre-explosion

* E-mail: alet@hartrao.ac.za

¹ Ergon et al. (2014) re-examined the various estimates of the distance to M51 to arrive at the value of $7.8_{-0.9}^{+1.1}$ Mpc, which is slightly lower than the value of 8.4 Mpc we had used in our earlier papers.

² The National Radio Astronomy Observatory is a facility of the National Science Foundation operated under cooperative agreement by Associated Universities, Inc.

Hubble Space Telescope (HST) images, but has since disappeared, has been identified as the progenitor (Van Dyk et al. 2013; Ergon et al. 2014). The progenitor’s main-sequence mass is estimated to around $13 M_{\odot}$ although the various workers give masses in the range of 10 to $19 M_{\odot}$ (Sahu, Anupama & Chakradhari 2013; Van Dyk et al. 2011; Maund et al. 2011; Bersten et al. 2012). It was an extended star with a radius of $200 \sim 300 R_{\odot}$ (Van Dyk et al. 2011; Bersten et al. 2012; Ergon et al. 2014). In addition, a blue companion to SN 2011dh’s yellow supergiant progenitor has also likely been detected in deep near-UV images obtained with the *HST* (Folatelli et al. 2014), making SN 2011dh the second core-collapse SN, after SN 1993J (Maund et al. 2004; Fox et al. 2014), to show strong evidence of a binary companion to the progenitor.

The size and expansion velocity of the shock front is a basic characteristic distinguishing different SNe, and it is therefore important to determine it observationally as directly as possible. VLBI observations are the most direct way of making this measurement (see e.g., Bietenholz et al. 2010; Brunthaler et al. 2010; Bietenholz 2008a). Unlike the optical emission, which mostly originates in the denser and more slowly moving inner ejecta, the radio emission generally traces the fastest ejecta. The radio emission is thought to originate in the region between the forward and reverse shocks. In the particularly well-studied case of SN 1993J, Bartel et al. (2007) show that there is a close relationship between the outer boundary of the radio emission and the location of the forward shock.

VLBI observations of SN 2011dh were first obtained at $t = 14$ d (2011 Jun 14, Martí-Vidal et al. 2011b). Although an accurate centre position was obtained, no useful constraint on the size could be obtained at this early epoch. Further VLBI observations were obtained at epochs $t = 83$ and 179 d (2011 Aug. 22 and 2011 Nov. 26) by Bietenholz et al. 2012 (see also Bietenholz et al. 2011). At both epochs, we used the the High Sensitivity Array (HSA), consisting of the NRAO VLBA, the Effelsberg telescope and the Robert C. Byrd Green Bank Telescope, and obtained useful measurements or upper limits on the source size. At $t = 83$ d we observed at 22 GHz, while at $t = 179$ d we observed at 8.4 GHz. At $t = 179$ d, the measured radius corresponds to an expansion velocity of $20000 \pm 6500 \text{ km s}^{-1}$ at 7.8 Mpc.

Aside from the relatively direct measurement using VLBI, the radius of the radio emitting region can also be determined from the radio spectral energy distribution (SED) if the spectrum is dominated by synchrotron self-absorption (SSA), as is generally expected at early times (see Chevalier & Fransson 2006). Soderberg et al. (2012) and Krauss et al. (2012) show that the radio spectrum of SN 2011dh was consistent with being dominated by SSA, and gave radius determinations up to $t = 92$ d. Although the calculation of the radius based on the SSA spectrum is fairly robust, it is more model-dependent than the more direct VLBI measurements. SN 2011dh represents so far the best example for directly comparing the radii of the shock wave determined in these two different fashions, and Bietenholz et al. (2012) show that for the measurements up to $t = 179$ d, there is excellent agreement between the two methods, thereby providing important confirmation for the radii derived from the SED by assuming SSA.

SN 2011dh was unusual in that it remained radio-bright

enough for VLBI observations for more than a year. We undertook a further epoch of VLBI observations, as well as observations to measure the total flux density with the VLA to determine the continued evolution of this SN, and we report on these results in this paper.

2 OBSERVATIONS AND RESULTS

2.1 VLA flux density observations and results

We observed SN 2011dh with the VLA to get a total flux density measurements at 8.4 GHz on 2012 Aug 1 (program 12A-286) and on 2014 Jan 31 (program 13A-370).

The 2012 Aug 1 observations were done with the array in the B configuration and we used a bandwidth of 1 GHz centred on 8.5 GHz. They were reduced using the NRAO’s Astronomical Image Processing System (AIPS), with the flux density scale being set from observations of 3C286 using the Perley-Butler 2010 coefficients. We measured an 8.5-GHz flux density of 0.88 ± 0.06 mJy, where the uncertainty includes the noise as well as an assumed 5% uncertainty in the flux density calibration.

The 2014 Jan 31 observations were done with the array in the BnA configuration and we used a bandwidth of 1 GHz centred on 7.1 MHz. They were reduced using AIPS, and calibrated to the same flux density scale using observations of 3C 286. We measured a flux density of 0.66 ± 0.035 mJy, where again the uncertainty includes the noise as well as an assumed 5% uncertainty in the flux density calibration.

In Figure 1 we show the 8.4-GHz radio lightcurve of SN 2011dh. We include the two new measurements described above as well as earlier ones taken from Bietenholz et al. (2012) and Krauss et al. (2012). The logarithmically interpolated value at the time of our VLBI observations (2012 Aug. 26) was 0.86 mJy. We scaled all the flux-density measurements taken between 7 and 9 GHz to 8.4 GHz using a spectral index of $\alpha = -0.7$ (where $S_{\nu} \propto \nu^{\alpha}$ Krauss et al. 2012). We are not sensitive to the exact value assumed for the spectral index: the earlier measurements, when the spectral index may have been notably different from -0.7 were taken at 8.4 GHz, and therefore required no scaling, and even in the most extreme case of the last measurement, at 7.1 GHz, a difference of 0.2 in the spectral index would change the plotted value by less than the uncertainty. Note that the decay has flattened with the flux density, $S \propto t^{-\beta}$ with $\beta \approx 1.17 \pm 0.13$ for $t < 159$ d to $\beta \approx 0.57 \pm 0.13$ for $t > 159$ d.

2.2 VLBI Observations

We obtained VLBI imaging observations of SN 2011dh using the high-sensitivity array, which consisted of the NRAO Very Long Baseline Array (VLBA; 10×25 -m diameter, distributed across the United States) and the NRAO Robert C. Byrd (~ 105 m diameter) telescope and the Effelsberg (100 m diameter) telescope. Due to a technical failure, the St. Croix VLBA telescope did not observe. The observations occurred on 2012 Aug 26, and lasted for a total of 13 hr. At the midpoint of our observing session the age of the SN was 453 days.

To measure the tropospheric zenith delay and clock offsets at each antenna we included three “geodetic blocks” of

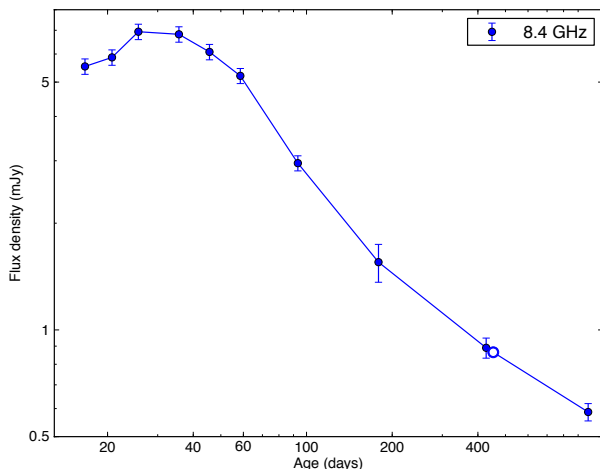


Figure 1. The 8.4-GHz lightcurve of SN 2011dh, as obtained from EVLA observations. Flux density measurements are shown by solid circles, and the logarithmically interpolated value at the time of our VLBI observations (0.86 mJy on 2012 Aug. 26) by an open circle. Details for the last two measurements are given in the text, and the remainder are taken or interpolated from Bietenholz et al. (2012) and Krauss et al. (2012). The age of the SN is calculated from the explosion date of 2011 May 31.6 UT.

~30 minutes each at the start, middle and end of our observations (see Brunthaler, Reid & Falcke 2005; Reid & Brunthaler 2004). In each of these geodetic blocks we observed 9–14 bright reference sources chosen from the International Celestial Reference Frame (ICRF) list of sources (Fey, Gordon & Jacobs 2009). For our geodetic blocks we recorded 8 intermediate frequencies covering a bandwidth of 8 MHz spread over a ~400 MHz range.

For the observations of SN 2011dh we recorded a contiguous bandwidth of 64 MHz in each of the two senses of circular polarization with two-bit sampling for a total bit rate of 512 Mbit s⁻¹. We used the same calibrator sources as in our previous VLBI observations of SN 2011dh. We used J1332+4722 (ICRF J133245.2+472222), which is 0.5° away from SN 2011dh, as our primary calibrator. This source is an ICRF source with a position known to ~70 μas (Fey, Gordon & Jacobs 2009). Any positions in this paper are calculated by taking the position of J1332+4722 to be Right Ascension (RA) = 13^h 32^m 45^s.24642, Declination (decl.) = 47° 22′ 22″.6670. We also obtained observations of the quasar, JVAS J1324+4743, about 1.5° away from J1332+4722, as an astrometric check source. The purpose of the observations of J1324+4743 was to check the quality of the phase-referencing and also to provide a second astrometric reference source to check the positional accuracy.

We used a cycle time of ~150 s, with ~110 s on SN 2011dh and ~40 s on J1332+4722. During the observing run we spent three ~20 m periods observing our astrometric check source, J1324+4743, using a similar phase-referencing pattern as we used for SN 2011dh.

The VLBI data were correlated with the DiFX correlator (Deller et al. 2011), and the analysis carried with AIPS. We corrected for the dispersive ionospheric delay using the AIPS task TECOR, and we solved for the zenith tropospheric delay on the basis of our geodetic-block observations. We discarded any SN 2011dh visibility data obtained when

either of two of the antennas involved was observing at elevations below 10°.

The initial flux density calibration was done through measurements of the system temperature at each telescope, and then improved through self-calibration of the primary reference source J1332+4722. This source is slightly resolved, as can be seen on the images in the VLBA calibrator list data-base³, and also from our previous observations at 22 and 8.4 GHz (Bietenholz et al. 2012). We see a similar structure in the image from our current observations at 8.4 GHz, where a weak extension or second component is visible ~2 mas to the west-southwest of the peak.

Our final amplitude and phase calibration was derived using a CLEAN model of this source, with the peak-brightness point in the image being placed at the nominal coordinates given above⁴. Finally this calibration was interpolated to the intervening scans of SN 2011dh.

2.3 VLBI Results

We detected SN 2011dh with good signal-to-noise ratio, and obtained a good VLBI image of SN 2011dh, with a resolution of 0.79 × 0.52 mas (FWHM), a dynamic range of 23, and an image background rms of 12 μJy beam⁻¹. We show the image in Figure 2. The total CLEAN flux density was 760 μJy beam⁻¹, which was ~90% of the total flux density measured using the VLA (see section 2.1). The structure of SN 2011dh is relatively circular at the lower contours, but with a clear detection of two hot-spots as evident in the image.

As in our previous VLBI observations (Bietenholz et al. 2011, 2012), we again turn to fitting a spherical-shell model, with an outer radius of 1.25× the inner radius, directly to the visibility measurements to accurately measure the size and centre position of the source. The free parameters in the fit are the centre position, the radius, and the flux density.

We take the fitted centre position of the model as our best estimate of the centre position of SN 2011dh. For the observations of SN 2011dh, at $t = 453$ d, the position of the model centre was RA = 13^h 30^m 5^s.105478 and decl. = 47° 10′ 10″.92261. The statistical uncertainty on this position is 30 μas in both RA and decl.

The fitted outer radius was 636 ± 29 μas. The statistical uncertainty was ±23 μas, and a Monte-Carlo simulation with 16 trials where we randomly varied the amplitude gains by $\sigma = 20\%$ gave an additional radius uncertainty due to possible amplitude calibration errors of 13 μas. We add these contributions in quadrature, and our final standard error on the fitted outer radius is therefore 29 μas. At 7.8 Mpc, this angular radius corresponds to a linear radius of $(7.4 \pm 0.3) \times 10^{16}$ cm, and an average expansion velocity since the explosion of 18900_{-2400}^{+2800} km s⁻¹.

³ <http://www.vlba.nrao.edu/astro/calib>

⁴ The deviation of the source geometry of J1332+4722 from a point source is small enough so that the effect of using a point model in the solutions for delay and delay rate made using FRING is negligible.

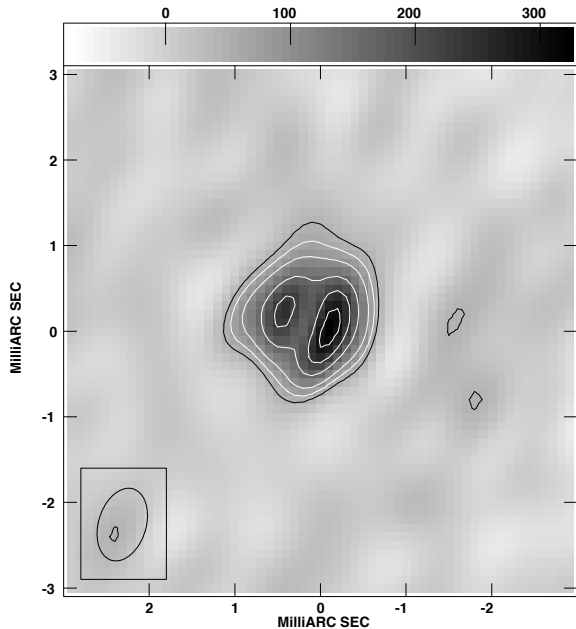


Figure 2. The 8.4-GHz VLBI CLEAN image of SN 2011dh on 2012 August 26, at $t = 453$ d. The contours are drawn at -12 , 12 , 20 , 30 , 50 (emphasized), 70 and 90% of the peak brightness, which was $270 \mu\text{Jy beam}^{-1}$. The convolving beam, indicated at lower left, was 0.79×0.52 mas (FWHM) at p.a. -15° . The image was made using robust weighting. The total CLEAN flux density was $760 \mu\text{Jy}$, and the background rms level was $12 \mu\text{Jy beam}^{-1}$. North is up and east is to the left.

3 DISCUSSION

We obtained phased-referenced VLBI observations of SN 2011dh, with the primary goal of obtaining a clearly resolved image of the expanding shell of ejecta, at $t = 453$ d after the explosion. We obtained a fairly well resolved image of SN 2011dh, shown in Fig 2, which shows a shell like structure that is fairly circular. Our image shows a bilateral enhancement of brightness, with hot-spots located approximately east and west along the ridge. In the case of the similar Type IIb SN, SN 1993J, there are clear time-dependent modulations of the brightness along the ridge-line which were larger than the noise or any systematic during the first two years (Bietenholz, Bartel & Rupen 2003; Bietenholz 2008b). Do the hot-spots in the image of SN 2011dh indicate a real brightness enhancement along the ridge? Even in the case of a completely circular structure, such a bilateral enhancement is in fact expected in the case of an elliptical CLEAN beam, with the hot-spots occurring at a p.a. at right angles to the elongation of the beam. We made simulated visibility data sets of a purely circular shell model with a noise level similar to that in the real data. When these were CLEANed in a fashion similar to the real data, the resulting images also tended to display hot spots, similar in brightness to those visible in Figure 2. We therefore conclude that although the bilateral enhancement seen in Figure 2 could be real, a perfectly uniformly circular structure is also compatible with the data.

We combined the present VLBI measurement of the centre position and outer radius with those from earlier ob-

servations from Bietenholz et al. (2012), Krauss et al. (2012) and Martí-Vidal et al. (2011b).

Since slightly different correlator positions for the phase-reference source J1322+4722 were used in the different VLBI experiments, we corrected the phase-referenced SN 2011dh centre position as well as that of the check source, J1324+4743, so that they are all relative to the position of J1322+4722 given in §2.2 above.

Since all three of our VLBI runs included observations of the check source, we can compare the phase-referenced position of J1324+4743 among the three epochs. We found that the scatter in this position over the three epochs was $130 \mu\text{as}$ in R.A. and $90 \mu\text{as}$ in decl. This scatter is larger than the expected astrometric errors, suggesting that there is some small apparent motion in one (or both) of the sources. Since we do not know whether our phase-reference source, J1324+4743, or the check source J1322+4722 has an apparently variable position, we take this scatter to be the uncertainty in the position of the phase-reference source. Based on this, we then take a conservative value of $130 \mu\text{as}$ for the uncertainty also in the centre position of SN 2011dh.

Turning now to the centre positions of SN 2011dh, and including the value at $t = 14$ d from Martí-Vidal et al. (2011b), we performed a least-squares fit of the position as a function of time. We find a proper motion of $55 \pm 66 \mu\text{as yr}^{-1}$ (at p.a. -15°), which corresponds to $2000 \pm 2400 \text{ km s}^{-1}$, with a 3σ upper limit of 9200 km s^{-1} .

We note that any proper motion due M51’s galactic rotation is expected to be only a few hundred km s^{-1} , well below our uncertainty, so we can take this projected speed to be that of SN 2011dh’s centre with respect to its local frame of rest within M51.

For the outer radius of the radio emitting region, which as we have argued, should be closely tied to the outer shock radius, we use the value determined in the present work along with the two VLBI values from Bietenholz et al. (2012), and those determined from the radio spectrum by assuming SSA from Krauss et al. (2012). We scale all the radii to a consistent distance of 7.8 Mpc. We plot them in Figure 3.

The expansion of a SN is usually parametrized as a power-law with $R = At^m$, where R is the radius, t is the time, m is the power-law index, called the “deceleration parameter” and A is the radius at $t = 1$. A weighted least-squares fit to all the values of R gives

$$R = (0.544 \pm 0.14) (t/30\text{d})^{(0.961 \pm 0.011)} \times 10^{15} \text{ cm}$$

All the radius measurements are consistent with a power-law evolution. The fitted expansion index $m = 0.961 \pm 0.011$ implies almost free expansion.

As already noted in Bietenholz et al. (2012), the radii measured with VLBI are consistent with those determined somewhat less directly from the SED under the assumption of SSA. The earlier VLBI radius measurements were rather more uncertain than those obtained from the SED. Our new measurement, by contrast, is rather more precise, and is still almost perfectly consistent with the powerlaw implied by the SED-based radius measurements. While it is possible that the SED-derived radii are systematically too small and that the expansion decelerated after $t \sim 100$ d we consider it an unlikely coincidence that the measured VLBI radius at $t = 453$ d would lie so close to the extrapolation of the pow-

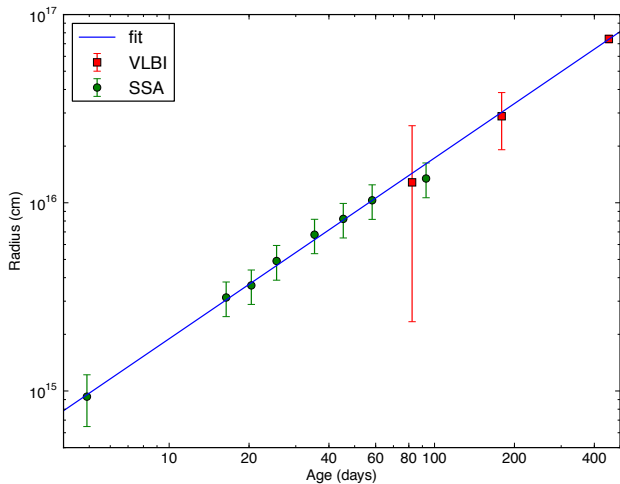


Figure 3. The shock front radii of SN 2011dh as estimated by two independent methods. Using red squares, we plot the values derived from fitting spherical shell models to the VLBI visibility-data from this paper and Bietenholz et al. (2012). The plotted 1σ error bars include statistical and systematic contributions (see Section 2.3 for details). It should be noted that the error bars on the last point are smaller than the point symbol and is therefore not visible in the plot. Using green circles, we plot the values calculated from the radio spectral energy distribution under the assumption that it is dominated by SSA (synchrotron self-absorption), with the radius values taken from Soderberg et al. (2012) and Krauss et al. (2012), again with uncertainties including statistical and systematic components. The blue line represents our power-law fit to all the values, with $R = 5.44 \times 10^{15} (t/30 \text{ d})^{0.961} \text{ cm}$ (see text).

erlaw seen at early times in that case. The consistency seen between the SED-derived radius measurements and those obtained from VLBI therefore provides strong validation for the method of calculating the shockfront radius from the SED under the assumption of SSA along the lines suggested by Chevalier & Fransson (2006).

The radii determined from the SED depend on $D^{(18/19)}$ whereas the (linear) radii measured with VLBI depend on D , so only very large errors in D would produce a substantial scaling between the two kinds of radius determinations. We note, however, that by comparing the angular expansion velocity as determined from VLBI and less directly from the SED fits, with linear expansion velocity measured from optical spectroscopy, a direct distance can be determined via the “expanding shock front” method. See Bartel et al. (2007). For an description of this method, and its application in the case of SN 1993J in M81. We defer a detailed comparison along these lines to a future paper, but note here that our fit implies an expansion velocity at $t = 30 \text{ d}$ of $20600_{-2400}^{+3000} \text{ km s}^{-1}$, where we include in the uncertainty the contribution due to the distance uncertainty ($7.8_{-0.9}^{+1.1} \text{ Mpc}$). This velocity compares very well to maximum velocity seen at the blue edge of $H\alpha$ absorption seen in the optical at the same age (e.g. Marion et al. 2014).

Comparing SN 2011dh to SN 1993J.

We can compare SN 2011dh to SN 1993J: both were of Type IIb, and had extended progenitors with binary companions,

and had lost a considerable fraction of their hydrogen envelopes to the companion before the SN explosion. The amount of radio emission as well as the deceleration are ultimately dependent on the energy dissipated as the shock ploughs out through the CSM, and depend therefore on the density profiles in the ejecta and the CSM. In particular, if the density profiles of the ejecta and the CSM are power-laws in radius, then a self-similar solution exists, and both the total flux-density and the shock radius follow power-laws in time (Chevalier 1982; Fransson, Lundqvist & Chevalier 1996). The flattening of SN 2011dh’s radio lightcurve decay after $t = 179 \text{ d}$ suggests a relative decrease in the circumstellar density (a relative increase in the ejecta density is also possible, but less likely at this early stage when the ejecta are in almost free expansion). If the CSM density is parametrized as $\rho_{\text{CSM}} \propto r^{-s}$, where $s = 2$ is the value expected of a steady wind, then the flattening of the flux density decay for SN 2011dh suggests a flattening of circumstellar density profile to $s < 2$ at radius of $\sim 3 \times 10^{17} \text{ cm}$. For a wind velocity of 10 km s^{-1} , this implies that the progenitors mass-loss rate decreased around 10000 yr before the explosion.

For SN 1993J, the radio lightcurves and expansion were particularly well determined (see, e.g. Bartel et al. 2002; Martí-Vidal et al. 2011a). SN 1993J was about four times as radio luminous as SN 2011dh, as the former reached a peak 8.4-GHz spectral luminosity of $\sim 2 \times 10^{27} \text{ erg s}^{-1} \text{ Hz}^{-1}$, compared to only $0.5 \times 10^{27} \text{ erg s}^{-1} \text{ Hz}^{-1}$ for the latter. The evolution of SN 1993J’s radio lightcurves was much slower than that of SN 2011dh, since the former reached an 8.4 GHz peak only after $t \sim 150 \text{ d}$, compared to the $t = 30 \text{ d}$ for SN 2011dh. However, we note that a circumstellar density profile flatter with $s < 2$, i.e. flatter than that of a steady wind, was also suggested for SN 1993J (e.g. van Dyk et al. 1994; Fransson, Lundqvist & Chevalier 1996), although models with a constant $s = 2$ can also reproduce the measurements (e.g. Fransson & Björnsson 1998; Martí-Vidal et al. 2011a).

Overall the fast rise of the radio lightcurve to its maximum, the small deceleration and the low peak luminosity imply that the CSM in the case of SN 2011dh was less dense than that of SN 1993J. Other Type IIb SNe which have shown shown similarly quick rise times and relatively low radio luminosities are SN 2008bo (Stockdale et al. 2008), and SN 2008ax (Roming et al. 2009), and indeed the similarities of SN 2011dh’s optical spectra to those of SN 2008bo have already been pointed out (Maund et al. 2011; Marion et al. 2014).

With our new VLBI image, SN 2011dh takes its place among the only six recent SNe for which resolved images of the ejecta are available, with the others being SN 1979C (Bartel & Bietenholz 2008), SN 1987A (Ng et al. 2011), SN 1986J (Bietenholz, Bartel & Rupen 2010), SN 1993J (Bietenholz, Bartel & Rupen 2003), SN 2008iz (Brunthaler et al. 2010). All of these SNe show an approximately circular shell structure, although modulations along the projected ridge-line of the shell are common. It will be important to obtain VLBI images of any future SNe which are sufficiently close and radio-bright to better establish the range of morphologies and understand the ejection process.

REFERENCES

- Arcavi I. et al., 2011, *ApJL*, 742, L18
- Bartel N., Bietenholz M. F., 2008, *ApJ*, 682, 1065
- Bartel N. et al., 2002, *ApJ*, 581, 404
- Bartel N., Bietenholz M. F., Rupen M. P., Dwarkadas V. V., 2007, *ApJ*, 668, 924
- Bersten M. C. et al., 2012, *ApJ*, 757, 31
- Bietenholz M., 2008a, in *The role of VLBI in the Golden Age for Radio Astronomy*. Online at <http://pos.sissa.it/cgi-bin/reader/conf.cgi?confid=72>, p.64
- Bietenholz M., 2008b, in *The role of VLBI in the Golden Age for Radio Astronomy*. Online at <http://pos.sissa.it/cgi-bin/reader/conf.cgi?confid=72>, p.64
- Bietenholz M. F., Bartel N., Rupen M. P., 2003, *ApJ*, 597, 374
- Bietenholz M. F., Bartel N., Rupen M. P., 2010, *ApJ*, 712, 1057
- Bietenholz M. F., Brunthaler A., Bartel N., Chomiuk L., Rupen M. P., Soderberg A., Zauderer B., 2011, *The Astronomer's Telegram*, 3641, 1
- Bietenholz M. F., Brunthaler A., Soderberg A. M., Krauss M., Zauderer B., Bartel N., Chomiuk L., Rupen M. P., 2012, *ApJ*, 751, 125
- Bietenholz M. F. et al., 2010, *ApJ*, 725, 4
- Brunthaler A. et al., 2010, *Astron. Astrophys.*, 516, A27
- Brunthaler A., Reid M. J., Falcke H., 2005, in *Astronomical Society of the Pacific Conference Series*, Vol. 340, *Future Directions in High Resolution Astronomy*, J. Romney & M. Reid, ed., p. 455
- Chevalier R. A., 1982, *ApJ*, 259, 302
- Chevalier R. A., Fransson C., 2006, *ApJ*, 651, 381
- Deller A. T. et al., 2011, *PASP*, 123, 275
- Ergon M. et al., 2014, *Astron. Astrophys.*, 562, A17
- Fey A. L., Gordon D., Jacobs C. S., eds., 2009, *IERS Technical Note*, Vol. 35, *The Second Realization of the International Celestial Reference Frame by Very Long Baseline Interferometry*. Frankfurt: Verlag des Bundesamts für Kartographie und Geodäsie, p. 1
- Folatelli G. et al., 2014, *ApJL*, 793, L22
- Fox O. D. et al., 2014, *ApJ*, 790, 17
- Fransson C., Björnsson C.-I., 1998, *ApJ*, 509, 861
- Fransson C., Lundqvist P., Chevalier R. A., 1996, *ApJ*, 461, 993
- Griga T. et al., 2011, *Central Bureau Electronic Telegrams*, 2736, 1
- Horesh A. et al., 2011, *The Astronomer's Telegram*, 3411, 1
- Horesh A., Zauderer A., Carpenter J., 2011, *The Astronomer's Telegram*, 3405, 1
- Krauss M. I. et al., 2012, *ApJL*, 750, L40
- Marion G. H. et al., 2011, *The Astronomer's Telegram*, 3435, 1
- Marion G. H. et al., 2014, *ApJ*, 781, 69
- Martí-Vidal I., Marcaide J. M., Alberdi A., Guirado J. C., Pérez-Torres M. A., Ros E., 2011a, *Astron. Astrophys.*, 526, A143
- Martí-Vidal I. et al., 2011b, *Astron. Astrophys.*, 535, L10
- Maund J. R. et al., 2011, *ApJL*, 739, L37
- Maund J. R., Smartt S. J., Kudritzki R. P., Podsiadlowski P., Gilmore G. F., 2004, *Nat*, 427, 129
- Ng C.-Y., Potter T. M., Staveley-Smith L., Tingay S., Gaensler B. M., Phillips C., Tzioumis A. K., Zandaro G., 2011, *ApJL*, 728, L15
- Reid M. J., Brunthaler A., 2004, *ApJ*, 616, 872
- Roming P. W. A. et al., 2009, *ApJL*, 704, L118
- Sahu D. K., Anupama G. C., Chakradhari N. K., 2013, *MNRAS*
- Silverman J. M., Filippenko A. V., Cenko S. B., 2011, *The Astronomer's Telegram*, 3398, 1
- Soderberg A. M. et al., 2012, *ApJ*, 752, 78
- Stockdale C. J., Weiler K. W., Immler S., Marcaide J. M., Panagia N., Pooley D., Sramek R. A., van Dyk S. D., 2008, *The Astronomer's Telegram*, 1484, 1
- Van Dyk S. D. et al., 2011, *ApJL*, 741, L28
- van Dyk S. D., Weiler K. W., Panagia N., Rupen M. P., Sramek R. A., 1994, *IAU Circ.*, 5979, 2
- Van Dyk S. D. et al., 2013, *ApJL*, 772, L32

This paper has been typeset from a \TeX / \LaTeX file prepared by the author.